

PIT Project

Behaviour of steel framed structures under fire conditions

**British Steel Fire Test1:
Analysis of results from BS/TEST1 model,
Part A: Slab grillage model**

Final Research Report

Report R99 AM1

Abdel Moniem Sanad

**The University of Edinburgh
School of Civil & Environmental Engineering
Edinburgh, UK**

December, 1999

TABLE OF CONTENTS

1. GENERAL NOTES	3
2. LIST OF FIGURES	3
3. INTRODUCTION	6
4. FLOOR DEFLECTION	7
5. AXIAL BEHAVIOUR OF THE HEATED BEAM	8
5.1. Behaviour near the connection	8
5.2. Behaviour inside the heated compartment	8
5.3. Global equilibrium	9
6. BENDING BEHAVIOUR OF THE HEATED BEAM	9
6.1. P-D moment during fire	9
6.2. Composite moment along the beam	10
7. BEHAVIOUR OF SLAB IN TRANSVERSE DIRECTION	10
8. GENERAL DISCUSSION	11
9. CONCLUSION	12
10. REFERENCES	13
11. FIGURES	14

1. GENERAL NOTES

In the description of the numerical model below the following terms are used :

1. “The plane” to define the plane of the floor.
2. “Joist” means a steel beam, and the test Joist means the heated Joist during the fire test.
3. “Vertical” means vertical to the slab plane.
4. “In plane” means in the plane of the Long. slab.
5. “Joist longitudinal direction” or “longitudinal direction” to mean parallel to the Joist length coordinate.
6. “Transverse direction” to mean at right angle to the Joist longitudinal direction (i.e. in the direction of the longitudinal axis of the ribs Figure 1).
7. “Reference vertical co-ordinate” is the interface between the Long. slab and Joist .

2. LIST OF FIGURES

A) General layout

Figure 1 : Layout of the Cardington fire test1.

Figure 2 : Layout of the finite element model

The following set of figures describes the evolution against time of deflections, axial forces and moment in different structural member :

B) Heated joist

Figure 3 : Joist thermal deflection at mid-span

Figure 4 : Axial force in Long. slab and joist at $x/l = 0$

Figure 5 : Axial force in Long. slab and joist at $x/l = 0.1$

Figure 6 : Axial force in Long. slab and joist at $x/l = 0.2$

Figure 7 : Axial force in Long. slab and joist at $x/l = 0.3$

Figure 8 : Axial force in Long. slab and joist at $x/l = 0.4$

Figure 9 : Axial force in Long. slab and joist at $x/l = 0.5$

Figure 10 : Composite axial force at mid-span and support

Figure 11 : Moment applied on composite beam

Figure 12 : Moment in Long. slab and joist at $x/l = 0$

Figure 13 : Moment in Long. slab and joist at $x/l = 0.1$

Figure 14 : Moment in Long. slab and joist at $x/l = 0.2$

Figure 15 : Moment in Long. slab and joist at $x/l = 0.3$

Figure 16 : Moment in Long. slab and joist at $x/l = 0.4$

Figure 17 : Moment in Long. slab and joist at $x/l = 0.5$

Figure 18 : Composite moment at mid-span and support

Figure 19 : Composite moment due to thrust at mid-span and support

Figure 20 : Moments carried by the composite beam

C) Slab in the transverse direction (Ribs)

Figure 21 : Rib axial force over the heated joist

Figure 22 : Rib moment over the heated joist

Figure 23 : Rib moment over the non heated joist

Figure 24 : Rib moment at far end

The next set of figures describes the space distribution of axial forces, and moment in different structural member during the fire :

D) Heated joist

Figure 25 : Composite axial force along the beam (20-850°C)

Figure 26 : Axial force along the Long. slab and joist at 20°C

Figure 27 : Axial force along the Long. slab and joist at 97°C

Figure 28 : Axial force along the Long. slab and joist at 191°C

Figure 29 : Axial force along the Long. slab and joist at 293°C

Figure 30 : Axial force along the Long. slab and joist at 393°C

Figure 31 : Axial force along the Long. slab and joist at 495°C

Figure 32 : Axial force along the Long. slab and joist at 612°C

Figure 33 : Axial force along the Long. slab and joist at 714°C

Figure 34 : Axial force along the Long. slab and joist at 816°C

Figure 35 : Axial force along the Long. slab and joist at 838°C

Figure 36 : Composite moments along the beam (20-850°C)

Figure 37 : Moments along the Long. slab and joist at 20°C

Figure 38 : Moments along the Long. slab and joist at 97°C

Figure 39 : Moments along the Long. slab and joist at 191°C

Figure 40 : Moments along the Long. slab and joist at 293°C

Figure 41 : Moments along the Long. slab and joist at 393°C

Figure 42 : Moments along the Long. slab and joist at 495°C

Figure 43 : Moments along the Long. slab and joist at 612°C

Figure 44 : Moments along the Long. slab and joist at 714°C

Figure 45 : Moments along the Long. slab and joist at 816°C

Figure 46 : Moments along the Long. slab and joist at 838°C

E) Slab in the transverse direction (Ribs)

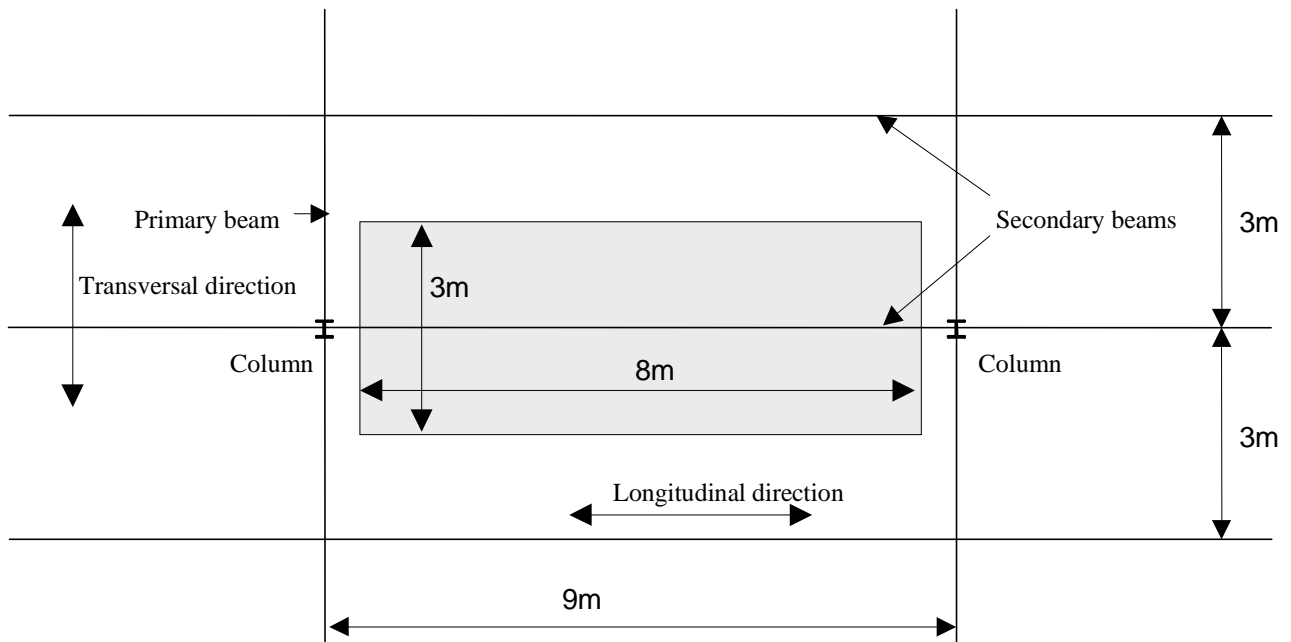
Figure 47 : Axial force in the rib crossing the joist at $x/l=0.5$

Figure 48 : Shear force in the rib crossing the joist at $x/l=0.5$

Figure 49 : Moment in the rib crossing the joist at $x/l=0.5$

3. INTRODUCTION

The results discussed in this report are obtained from the finite element model developed at the University of Edinburgh (Sanad *et al.* 1999)⁸ using the commercial software ABAQUS¹. The geometry of the test is given in Figure 1 and the layout of the finite element model is given in Figure 2. The test is fully described in (Kirby 1995)⁷. Test 1 was performed on the seventh floor of the building and the fire compartment was arranged to study the behaviour of a secondary beam spanning between two columns. The dimensions of the compartment were 8m×3m. The tested beam had a span of 9m, and was connected to columns at both ends. A standard composite profiled deck slab was used to span the 3m between equally spaced secondary beams supported either from primary beams or columns (Bravery 1993)². The slab was cast in-situ on profiled steel decking and had a total thickness of 130mm. The thickness of the steel deck used is 9mm and the reinforcement consists of one layer of A142.



Layout of the Cardington Fire tests

Figure 1

The finite element model was fully described in (Sanad 1999)¹⁰. Figure 2 shows the layout of half the test compartment where the tested joist spanning 9m between two columns and the slab ribs crossing it at different locations. In the following section a discussion of the structural behaviour during the test is given based on the output obtained from the numerical model. The main forces and moment plotted for the tested joist and the slab were obtained directly from calculation. The composite forces and composite moment were subject to a more elaborated data processing. The composite axial force over the beam is the sum of the axial force in the joist and the composite longitudinal slab connected to it. The composite moment was divided to two part, the first is the sum of the moment acting on each member (joist and Long. slab) separately and the second part, due to the axial force in each member was obtained by calculated as the difference of the joist thrust and the slab thrust multiplied by the lever arm between the point of application of the two forces

(centroid of each element). For all figure a reference temperature was chosen to illustrate the level of heat reached by the structure at this stage of fire. The reference temperature is the temperature of the hottest steel region within the fire compartment, this was measured on the lower flange of the tested joist at mid-span and thus this temperature is used in our text as the reference temperature.

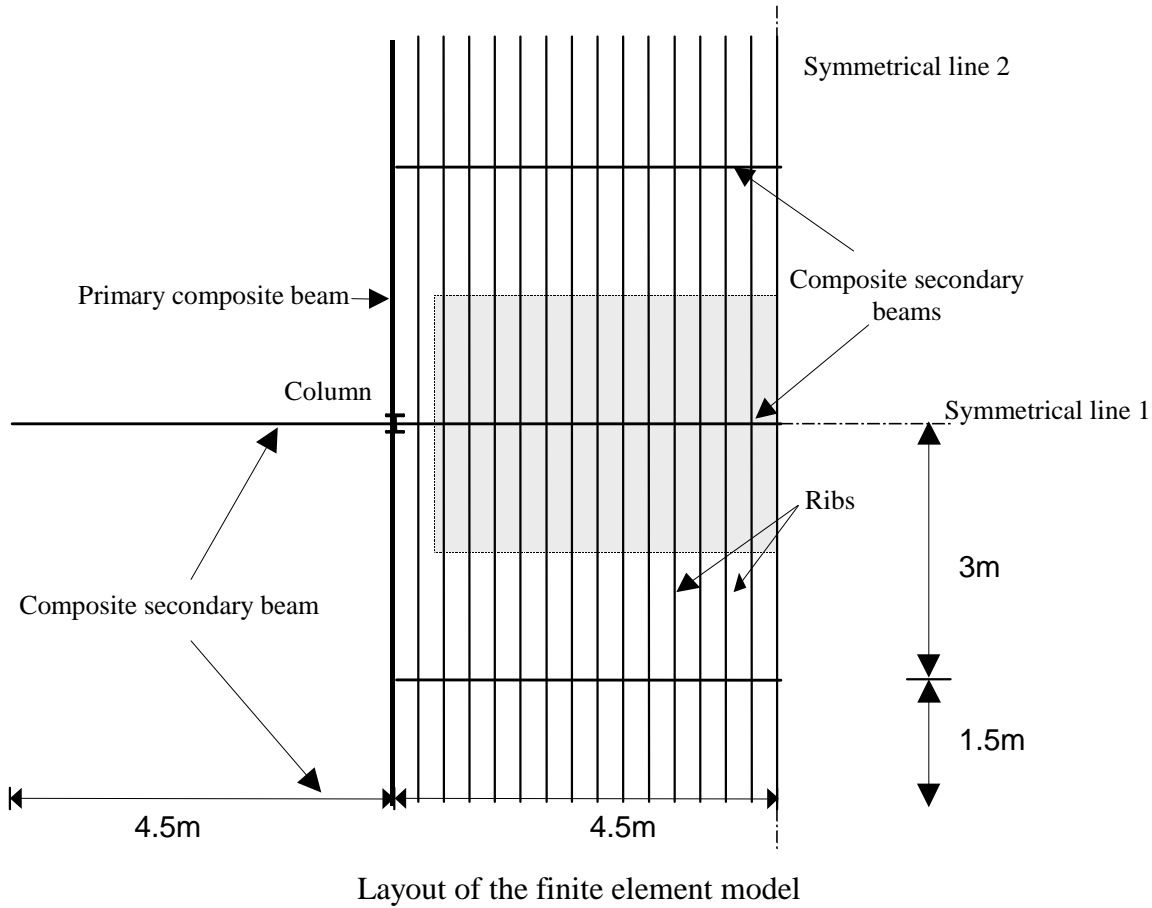


Figure 2

The analysis of internal generalised stresses in the structure are necessary here in order to give the full description of the local and global behaviour. A description of the structural behaviour according to the calculations undertaken is given below and compared where possible with the experimental observations.

4. FLOOR DEFLECTION

The main characteristic of the behaviour of the floor is the homogeneous deflection obtained over the full heated area. The maximum deflection is obtained at mid-span as shown in Figure 3. The deflection-temperature relationship is very close to a straight line with local perturbation due to the localised variation in the temperature-time heating regime. The value obtained for the deflection of the floor system at different locations (4 points along the beam) were in good agreement with the test measurements.

The axial forces in the joist and the longitudinal slab during the fire are plotted against the reference temperature at different location of the joist ($x/l=0, 0.1, 0.2, 0.3, 0.4, 0.5$). This axial forces are

shown in Figure 4 to Figure 9. On the same figures, the joist's ultimate forces were plotted to show the magnitude of the axial forces developed in the joist against its yield capacity.

5. AXIAL BEHAVIOUR OF THE HEATED BEAM

The behaviour of each structural element is self-explanatory and can be observed from the set of figures included in this report. This section discusses the behaviour of each structural element separately and is followed by a more general discussion based on the global equilibrium of the floor system and the contribution of each element to the equilibrium state.

5.1. Behaviour near the connection

In Figure 4, the axial thrust in the joist at the column end is plotted against the chosen reference temperature of the joist lower flange at mid span. The elastic axial force capacity of the joist at this location can be defined based on the first yield and ultimate stresses obtained from the stress-strain relationship. Because the material degradation of the steel does not affect the ultimate stress value until 400°C and the final temperature reached in the joist outside the compartment was 220°C, the ultimate capacity of the joist near the column does not drop during the entire heating regime, however the first yield value drops slightly. In Figure 4, the joist is initially in compression and the slab is in tension due to the hogging moment applied on the composite section at the column end. When the fire starts, the thermal expansion of the joist is restrained at this location giving rise to internal axial force, this compression force increases linearly and reaches the first deflection point (A) at 150°C. At this point, the axial force acting on the section reaches the first yield surface ($F_y' = \sigma_y' A_j$); and plastic strains start to accumulate in the joist. Beyond point A, a small increase in the joist force at this location is noticed due to the material hardening. The yielding of the joist at this section explains the first pattern obtained in the beam composite force (Figure 10), which is characterised by a linear increase of the axial strain from 0 to 150°C, followed by a flat stable axial strain representing the first yielding of the section.

5.2. Behaviour inside the heated compartment

Another key section was found to be the one just inside the compartment at $x/l=0.1$. At this location the temperature reaches 800°C at the end of the heating regime. Figure 5 shows the axial force during the fire against the yield and ultimate axial force capacity of the section, calculated according to the joist temperature at this location. The evolution of the thrust in the joist shows a similar behaviour as for the first section, characterised by linear increase to 150°C and a roughly constant value from thereon to 500°C. At this temperature the thrust in the joist hits the ultimate yield surface, and the behaviour from this point until the end of the fire is dominated by the material degradation. It may be noted here that the ultimate curve shown in the figure represents only the axial plastic limit of the section without considering the effect of the moment. This plastic surface should decrease if the effect of the section moment acting on the section is considered. However this comparison shows clearly that the third pattern of behaviour measured by the strain gauges, characterised by a non-linear decrease of the joist axial strain beyond 500°C until the end of the heating, is directly related to this event. The above phenomenon was characterised in the test by the buckling of the joist web at this location near 500°C. In the model the effect of this failure was reproduced by the plastification through the depth of the section.

Figure 6 to Figure 9 show similarly the evolution of the axial force in the joist and the slab during the fire at $x/l=0.2, 0.3, 0.4$ and 0.5 , at these sections the initial forces confirm the bending behaviour of the composite, where at mid-span (Figure 9) for example, the beam is in tension and the slab in

compression indicating a sagging moment acting on the beam at this section. However from the beginning of the fire all axial forces in the joist and the slab are dominated by the huge effect of restraint thermal expansion and both section go into higher compression regime.

5.3. Global equilibrium

Here the discussion is extended to study the global equilibrium in the longitudinal direction of the composite member. For the composite beam, the horizontal equilibrium condition means that the sum of the axial forces acting on the composite member shall be equal to zero. In Figure 10 the axial forces acting on the composite beam is represented by two curves for the section at the column and at mid-span. The two curves are very close to each other, showing that each section across the beam is subjected to the same compressive normal force (Figure 25).. The shape of the curve during the fire shows a linear increase of the thrust up to 150°C, due to the restrained thermal expansion of the composite member at the column end. From 150°C to 500°C another increase of thrust is observed with a smaller slope. Beyond 500°C a non-linear decaying trend is obtained until the end of the fire. As can be seen, the global equilibrium of the composite member is controlled by the local degradation of the joist sections, the first point is directly related to the first buckling of the section at the column and the second deflection point coincides with the plastification of the section inside the compartment. For axial force diagram over the composite beam is also given in detail at different instants during the fire (Figure 26 to Figure 35) showing the individual contribution of the joist and the Long. slab to the composite axial force.

6. BENDING BEHAVIOUR OF THE HEATED BEAM

6.1. P-D moment during fire

The increasing thrust developed in the composite beam during the fire combined with its deflection produces a second order moment which is called P-Δ. At ambient temperature the value of this moment is one order of magnitude less than the typical *ambient* moment due to the distributed load ($\frac{wl^2}{8}$), thus it is usually ignored for calculation as well as for design. Under increasing temperature

the magnitude of the P-Δ moment increases significantly as both P increase and Δ increases and in reality exceeds the initial moment at early stage of the fire (in this case at 300°C as shown in Figure 11). This new self implied moment can be defined as a new *thermal imposed* moment which depends on the axial restraint condition of the beam. Also the thermal gradient across the composite section (difference of temperature between the composite slab and the joist) imposes a thermal curvature over the section. When combined with a rotational restraint this imposed curvature produces a hogging moment over the length of the composite beam (temperature of steel joist is higher than composite slab temperature).

Under the new added *thermal* loads, the composite beam behaves accordingly to satisfy the equilibrium conditions and to carry both (*thermal* and *ambient*) loads. Figure 12 to Figure 17 show the moment acting on the joist and the slab separately at different section ($x/l=0.1$ to $x/l=0.5$). The same figures show also the yield and ultimate moment capacity of the joist at each location. Two major points can be noticed from these figures. First the moment in the slab is almost negligible compared to the moment in the joist at the same location. Second the moment in the joist near to mid-span are beyond the first yield from 450°C onward and are very close to the ultimate-softening curve of the joist moment capacity. This shows that from nearly 500°C till the end of the fire the joist is actually in a yielding state.

6.2. Composite moment along the beam

For bending moment diagrams over the composite beam is given in detail at different instants during the fire (Figure 36). The individual contribution of the joist and the Long. slab to the composite moment are given on the Figure 37 to Figure 46. The following discussion cover in the moment over two separate sections of the beam. Figure 18 shows the moment acting on two critical sections at support and mid-span. The curves show that initially the end section is under hogging moment and the mid-span is subjected to sagging which is a classic figure of a fixed end beam subjected to a distributed load. At the beginning of the fire (0-150°C) the moment at both sections (and in reality over the whole beam) is subjected to an increasing hogging moments. At 150°C the joist reaches its axial yield at end and consequently the composite moment over the section at this location reaches a limit up to 500°C. The capacity of the composite section is known to be larger in sagging then in hogging this can be observed from the same figure where the moment at mid-span increases from 150°C to 300°C then stabilises to 500°C. This increase of the moment at mid-span represent a redistribution of moment over the beam which is developed mainly to carry the increasing P-Δ moment. From 550°C to the end of fire the moment over the two sections (mid-span and end) reduce due to the joist failure (softening) inside the fire compartment.

Figure 19 shows the composite moment acting over the previous two sections. The same figure shows as part of the total composite moment the moment due to the thrusts in joist and Long. slab. As can be see from the curve, the largest part of the composite moment developed in over the beam are in fact due to the difference in thrust between the two individual members. When considering the beam as one single structural element, the different of moment between the end and mid-span can represent the total moment carried by the beam, this is represented by the first curve on Figure 20. At 20°C, the moment carried by the beam is due to only the *ambient* load this value is more or less constant up to 150°C as at beginning of the fire the magnitude of the *thermal* loads is relatively small (the sagging moment due to P-Δ is small and the hogging moment due to the thermal gradient is constant over the whole length of the beam). Then the beam carries an increasing extra load up to 300°C, then it reaches its capacity and carries a constant load up to 500°C then decreases till the end of the fire. The second curve on the same figure show the net moment acting on the beam (the total moment carried by the beam minus the P-Δ moment represented by the third curve). This second curve show the contribution of the composite beam to the total equilibrium of the floor, where a positive sign indicates the beam contributing positively to carry the floor and a negative sign shows that the beam is applying load to the rest of the structure. This is the case, as shown in the figure, from 550°C till the end of the fire where the heated composite doesn't contribute to support the floor contrarily it imposes load on it. The equilibrium of the floor at this stage is ensured by another load carrying mechanism as described in the following section.

7. BEHAVIOUR OF SLAB IN TRANSVERSE DIRECTION

Figure 21 shows the axial forces developed in the slab ribs in transverse direction at different location above the heated beam ($x/l=0.1$ to $x/l=0.5$). At ambient temperature this membrane forces are negligible. From 20°C to 200°C all the ribs are subjected to and increasing compressive forces as they expand against the cold surrounding slab. The magnitude of the compressive force developed in each rib depends on it location as can be seen from the figure. The axial force developed in each rib depends on the rib's location, the ribs near to the primary beam are subject to higher compression as they deflect less. The ribs at mid-span will be subjected to lower axial forces as they deflect more. From 150°C the axial forces developed reduces in all ribs with the ribs at mid-span ($x/l=0.4$ and $x/L=0.5$) going into tension from 500°C onward. This shows clearly that tensile

membrane forces are developed in the transverse direction of the slab at the later stages of the fire. This tensile membrane action is mobilised by compatibility of deflection in the longitudinal and transverse directions to carry the loads at later stage of the fire. This figure coincide exactly with the observation from Figure 20 where at this temperature the composite beam start applying loads to the rest of the structure. To be noticed here that the magnitude of the tensile forces developed in the transverse slab are far from the tensile capacity of the slab used here.

Figure 22 shows the moment developed in the ribs over the joist at the above locations. At ambient temperature all ribs are under hogging bending moment showing that the ribs are supported by the test beam at ambient temperature. Figure 23 and Figure 24 show also that at ambient temperature the ribs a subjected to a hogging moment over the parallel non-heated joists while the far end of the ribs, located at mid-span between two beams, is subject to a sagging moment. In this configuration the ribs are acting as continuous beam running over intermediate support and subjected to a distributed load. During the fire this configuration changes as can be seen from the figures. The ribs near the primary beams reach some yield line, over the heated joist, from nearly 200°C until the end of fire. For the ribs near the mid-span ($x/l=0.4$ and $x/l=0.5$), the hogging moment over the heated joist reduces with temperature increase, showing that less support is given by the heated joist during the fire and goes into sagging moment at the later stage of fire (350°C at $x/l=0.5$ and 520°C for $x/l=0.4$). This show clearly that the support given from the heated beam reduces during the fire. Over the next non heated secondary beams the hogging moment increase in all ribs with a larger effect for the ribs at $x/l=0.5$. which shows that the support coming from the non-heated beams increase during fire to compensate for the loss of support from the heated one.

The above conclusion can be clearly identified from the Figure 47 to Figure 49 where the axial force, shear force and bending moment diagrams are plotted along the mid-span rib for different times during the fire. To be noticed on Figure 48 that the magnitude of the reaction force obtained from the heated beam (showing here by the difference in the ribs shear between the left and right sides of the beams) reduces during fire and change signs between 700°C and 800°C of the reference temperature.

8. GENERAL DISCUSSION

The structural behaviour of the beam during the test showed rather a linear relationship between the deflection and the temperature at mid-span. The information obtained from the strain gauges gives an indication of the strain evolution during the fire. However these pieces of information are insufficient to understand the local behaviour at each section. The numerical model was able to reproduce the different patterns of behaviour obtained during the test, and the detailed investigations of the model results showed clearly that many different non-linear phenomena occur during the fire. These non-linearities do not seem to perturb much the deflection of the beam, nevertheless they are indispensable in explaining the global behaviour which is controlled by the local events at different sections of the composite member.

Some comments on the behaviour and the location of sections expected to yield seems necessary at this point. The location of the yielding section can be defined as related to two major factors; the material degradation due to high temperature and the location of most critical sections at ambient temperature due to the restraint conditions. The first is always inside the heated compartment, the second one is either at mid span, where the joist would yield in tension, or at the fixed end where it

shall yield (buckle) in compression. However during fire, the restrained expansion of the member produces a compression force in the joist and the failure in tension at mid-span can be excluded. Thus the second section expected to yield is always located at the column end. When the total length of the beam is heated the two sections coincide and the location of the critical section is obviously at the column. This was clearly found in three of the tests carried on the Cardington building, where local buckling was always observed near the connections. When the connection is outside the heated compartment, as it is the case for test1, the above two sections are situated at two different locations. The section near the fixed end is very probable to reach its first yield at the column. Although it is partially heated, and the second section is located where the maximum thrust exists inside the compartment, thus at the limit of the heated zone. However the local decline of the member at these locations does not affect greatly the global deflection and stability of the building but it affects considerably the redistribution of the internal forces in the structure. Under fire condition new *thermal* loads are self implied on the structure and different load carrying mechanism are mobilised to carry the extra loads. This load carrying mechanism are mainly developed through a moment redistribution toward the mid-span of the beam and through tensile membrane action in the slab. The later is developed through compatibility of deflections in the longitudinal and the transverse direction. This shows clearly that the problem treated here (test1) is a 3D problem which depends crucially on the displacements compatibility in the longitudinal and transverse directions.

9. CONCLUSION

The analysis of the results of the FE model developed at the university of Edinburgh (Sanad 1999)¹³, revealed important information concerning the structural behaviour of restrain composite beams under fire conditions. First the numerical model was able to follow the behaviour of the restrained composite beam of BS Test1 to the highest temperature attained by the fire. The predictions were then compared with experimental measurements of three different quantities: deflections, horizontal displacements and strains, each at a different location in the test, and both within and outside the heated zone. These comparisons showed that relatively good agreement has been achieved between the predictions and the test measurements at all times during the fire (Sanad et al.)¹³.

The different phenomena occurring during the fire were reproduced in the numerical model and the different patterns of behaviour were predicted. Other aspects of the structural behaviour which can not be verified against test observations were also obtained from this analysis. These may be regarded as reliable measures of the real behaviour. The analysis of the generalised stresses obtained from the numerical model revealed the reasons behind some observed phenomena, and explained the relationship between the global behaviour of the composite member and the local yielding of the joist at different locations. The discussion of the local and global behaviour of the beam showed that some sections of the joist reach the first yield at temperature as low as 150°C, and the joist reaches its ultimate capacity at other sections near 500°C. The analysis of the equilibrium of the composite beam showed that a very large P-Δ moment is developed at high temperature. Its value can exceed the value of the moment due to *ambient* loads. This shows clearly that axial restraint to thermal expansion should be considered in the design of the composite beam as an important loading condition to ensure that the design is safe under fire. However to establish a more coherent design rules the redistribution of extra moment and the large capacity of the composite beams together with the tensile capacity of the slab have to be taken into consideration as a load carrying mechanisms.

10. REFERENCES

1. Abaqus (1994), "Abaqus theory manual and users manual, version 5.4, Hibbit, Karlsson and Sorensen Inc., Pawtucket, Rhode Island, USA"
2. P.N.R. Bravery (1995), "Cardington large building test facility, Construction details for the first building, internal report British Steel plc."
3. D.J. O'Connor and al. (1995), "Determination of the fire endurance of model concrete Long slabs using a plastic analysis methodology, The Structural Engineer, Volume 73, No 19/3." (1995)
4. Eurocode 2 (1995), "Design of concrete structures Part1 2 : General rules Structural fire design, ENV 1992 1 2."
5. Eurocode 3 (1995), "Design of steel structures Part1 2 : Fire resistance, ENV1993 1 2."
6. Eurocode 4 (1994), "Design of composite steel and concrete structures Part1 1 : General rules and rules for buildings, ENV 1994 1 1"
7. B.R. Kirby (1995): Behaviour of a multi storey steel framed building subject to natural fires: Test1 restrained beam, deflection measurements, Document ref; S423/1/Part D1, British Steel plc.
8. Rotter, J.M., Sanad, A.M., Usmani, A.S. and Gillie, M. (1999) "Structural performance of redundant structures under local fires", Proc., Interflam '99, 8th International Fire Science and Engineering Conference, Edinburgh, 29 June - 1 July, Vol. 2, pp 1069 - 1080.
9. Sanad, A.M., Rotter, J.M., Usmani, A.S. and O'Connor, M.A. (1999) "Finite element modelling of fire tests on the Cardington composite building", Proc., Interflam '99, 8th International Fire Science and Engineering Conference, Edinburgh, 29 June - 1 July, Vol. 2, pp 1045 - 1056.
10. Sanad A.M. (1999) "British Steel Fire Test1: Reference ABAQUS model using grillage representation for slab" Research report R99-MD1, University of Edinburgh, Department of Civil and Environmental Engineering.
11. Sanad, A.M., Lamont, S., Usmani, A.S. And Rotter, J.M. (2000) " structural behaviour in fire compartment under different heating regimes – part 1 (Slab thermal gradients)" Fire Safety Journal, accepted for publication May 2000.
12. Sanad, A.M., Lamont, S., Usmani, A.S. And Rotter, J.M. (2000) " structural behaviour in fire compartment under different heating regimes – part 2 (Slab mean temperatures)" Fire Safety Journal, accepted for publication May 2000.
13. Sanad A.M., Rotter J.M., Usmani A.S. and O'Connor M.A. (2000), "Composite beams in large buildings under fire – numerical modelling and structural behaviour", Fire Safety Journal, accepted for publication June 2000.

11. FIGURES